arXiv:cond-mat/0012213v2 [cond-mat.dis-nn] 10 Jan 2001

Intermediate liquid-solid regime near the quantum melting of a two dimensional Wigner molecule

Georgios Katomeris and Jean-Louis Pichard
CEA, Service de Physique de l'Etat Condensé, Centre d'Etudes de Saclay, 91191 Gif-sur-Yvette, France

For intermediate values of the Coulomb energy to Fermi energy ratio r_s, the ground state of a few spinless fermions confined on a two dimensional torus is the quantum superposition of a floppy Wigner molecule with delocalized vacancies and of a Fermi liquid of intersticial particles. This raises the question of the existence of an unnoticed liquid-solid phase between the Fermi liquid and the Wigner crystal for fermionic systems in two dimensions.

PACS: 73, 73.20.-r, 73.21.-b, 67.80.-s

An outstanding question in quantum condensed matter is to know if the solid and the fluid can coexist in an intermediate phase separating the solid from the liquid. Such a phase was suggested [1] if the zero point motions of certain defects become sufficient to form waves propagating inside the solid. The defects of the crystalline solid can be simple vacancy-intersticial pairs or more complex excitations. Their statistics coincide with the statistics of the particles out of which the solid is made. For bosons, they may form a condensate, giving rise to a superfluid coexisting with the solid. This supersolid phase is discussed in certain bosonic models [2]. For fermions, the defects may form a Fermi liquid [3] coexisting with the solid, such that the system is neither a solid, nor a liquid. Two kinds of motion are possible in it; one possesses the properties of motion in an elastic solid, the second possesses the properties of motion in a liquid.

We study such a possibility for electrons created in a two dimensional ($2d$) heterostructure. Our motivation is threefold. First, it becomes possible to create very dilute $2d$ gases of electrons or holes in field effect devices and to vary by a gate the carrier density n_s such that the Coulomb energy to Fermi energy ratio $r_s \propto {n_s}^{-1/2}$ can reach high values where the charges become strongly correlated. The studied devices use doped semi-conductors [4] (Si-Mosfet, Ga-As heterostructures, Si-Ge quantum wells) or undoped organic crystals [5]. Since charge crystallization is expected for $r_s \approx 37$ in a clean system [6] and at lower r_s in the presence of impurities [7,8], to study in those devices how one goes from a Fermi liquid (low r_s) towards a Wigner crystal (large r_s) becomes possible. Second, the observation [4] of a metallic behavior at low temperatures in those systems raises the question of a possible intermediate phase, which should be neither a Fermi system of localized particles (Anderson insulator), nor a correlated and rigid solid of charges (pinned insulating Wigner crystal). Third, an unexplained intermediate regime was numerically observed [8,9] in small disordered clusters. Those studies give a first threshold r_s^F above which the Hartree-Fock (HF) approximation does not describe [10] the persistent currents driven by an Aharonov-Bohm flux ϕ. For $r_s < r_s^F$, the local currents are oriented at random by the impurities, while for $r_s > r_F$ they align [8,9,11] along the shortest direction enclosing ϕ. r_s^F is followed by a second threshold r_s^W where charge crystallization occurs and the persistent currents vanish. This intermediate regime characterizes the ground state and the low energy excitations and disappears when the excitation energy exceeds [9] the Fermi energy. Both numerics and experiments give an unexplained behavior restricted to temperatures smaller than the Fermi temperature for similar intermediate values of the ratio r_s.

Since the low energy levels do not obey [9] Wigner-Dyson statistics, the existence of non chaotic low energy collective excitations due to the interplay between the kinetic energy and the Coulomb repulsion in the clean limit can be suspected. For this reason, we have studied the same cluster than in Refs. [8,9] without random substrate and we have observed for intermediate values of r_s a liquid-solid regime of a type conjectured by Andreev and Lifshitz. The transfer of a charge from a crystal site towards some intersticial site creates a vacancy-intersticial pair. This costs an energy ϵ_0, but the pair can tunnel to give rise to a band of delocalized excitations of width t_0. Near the melting point of the crystal, t_0 may exceed ϵ_0 and the Wigner solid may co-exist with a liquid of delocalized defects. This picture is supported by an analysis of the ground state (GS) using a combination of Slater determinants (SDs) built out from plane waves and from site orbitals. The plane wave SDs are given by some excitations of the non interacting system and correspond to an excited liquid. The site SDs describe the Wigner solid molecule which dominates at large r_s. For $r_s^F \approx 9.31 < r_s < r_s^W \approx 27.93$ in the studied cluster, the GS is given by a quantum superposition of an excited liquid and of a Wigner solid. The structure of the low energy excitations, the errors made assuming certain truncations of the Hilbert space and the responses to small perturbations confirm the existence of two thresholds r_s^F and r_s^W between which unusual behaviors occur.

We consider N spinless fermions free to move on a square $L \times L$ lattice with periodic boundary conditions (BCs). As in Refs. [8,9], we take $N = 4$ and $L = 6$, the size $N_H = 58905$ of the Hilbert space being small enough to exactly diagonalize the Hamiltonian:

$$H = -t \sum_{<i,j>} c_i^\dagger c_j + U \sum_{i \neq j} \frac{n_i n_j}{2 r_{ij}} \tag{1}$$

using Lanczos algorithm. $c_i^\dagger$ (c_i) creates (destroys) a spinless fermion in the site i, t is the hopping term between nearest neighbors and r_{ij} is the shortest inter-particle distance in a lattice with periodic BCs. $n_i = c_i^\dagger c_i$ and the interaction strength U yields a Coulomb energy to Fermi energy ratio $r_s = U/(2t\sqrt{\pi n_s})$ for a filling factor $n_s = N/L^2 = 1/9$.

The system remains invariant under rotation of angle $\pi/2$ and under translations and reflections along the longitudinal x and transverse y directions. Invariance under translations implies that the momentum K is a good quantum number which remains unchanged when U varies. The symmetries imply that the states are fourfold degenerate if $K \neq 0$ and can be non degenerate if $K = 0$.

When $U = 0$, the states are N_H plane wave SDs $d^\dagger_{k(4)} d^\dagger_{k(3)} d^\dagger_{k(2)} d^\dagger_{k(1)} |0>$ ($d^\dagger_{k(p)}$ creating a particle in a state of momentum $k(p) = 2\pi(p_x, p_y)/L$), $|0>$ being the vacuum state and $p_{x,y} = 1, \ldots, L$). K_i and D_i being the momentum and the degeneracy of the states of energy E_i, the GSs ($E_0(U = 0) = -13t, K_0 \neq 0, D_0 = 4$) are followed by two sets of excitations ($E_1(U = 0) = -12t, D_1 = 25$) and ($E_2(U = 0) = -11t, D_2 = 64$). We denote $|K_0(\beta)>$ ($\beta = 1, \ldots, 4$) the SDs of energy $-13t$ and of momenta $K = (0, \pm\pi/3)$ and $(\pm\pi/3, 0)$ and $|K_1(\beta)>$ the 4 SDs of energy $-12t$ and of momentum $K_1 = 0$. For the non interacting system, the $|K_0(\beta)>$ are 4 orthonormal GSs and the $K_1(\beta)$ are 4 orthonormal first excitations, corresponding to a particle at an energy $-4t$ with $k(1) = (0, 0)$, two particles at an energy $-3t$ and a fourth particle of energy $-2t$ with momenta such that $\sum_{j=2}^{4} k(j) = 0$. One has $k(2) = (0, \pm\pi/3)$, $k(3) = (\pm\pi/3, 0)$ and $k(4) = (\mp\pi/3, \mp\pi/3)$ or $k(2) = (0, \mp\pi/3)$, $k(3) = (\pm\pi/3, 0)$ and $k(4) = (\mp\pi/3, \pm\pi/3)$.

When $t = 0$, the states are N_H Slater determinants $c_i^\dagger c_j^\dagger c_k^\dagger c_l^\dagger |0>$ built out from the site orbitals. The configurations $ijkl$ correspond to the N_H different patterns characterizing 4 different sites of the $L \times L$ square lattice. If we order the configurations by the smallest distance d between two sites, N_d denoting the number of configurations with inter-particle spacings larger than d, one has $N_1 = 27225, N_{\sqrt{2}} = 9837, N_2 = 2709, N_{\sqrt{5}} = 81$ configurations out of 58905 configurations. The $N_{\sqrt{5}}$ configurations have the smallest electrostatic energies, and contain 9 square configurations $|\Box_I>$ ($I = 1, \ldots, 9$) of side $a = 3$ (energy $E_0(t = 0) \approx 1.80U$), 36 parallelograms of sides $(3, \sqrt{10})$ (energy $\approx 1.85U$) and 36 other parallelograms of sides $(\sqrt{10}, \sqrt{10})$ (energy $\approx 1.97U$). Ordering the site configurations by increasing electrostatic energy, those 81 configurations are followed by 144 configurations obtained by moving a single site of a square configuration by one lattice spacing (deformed squares of energy $\approx 2U$).

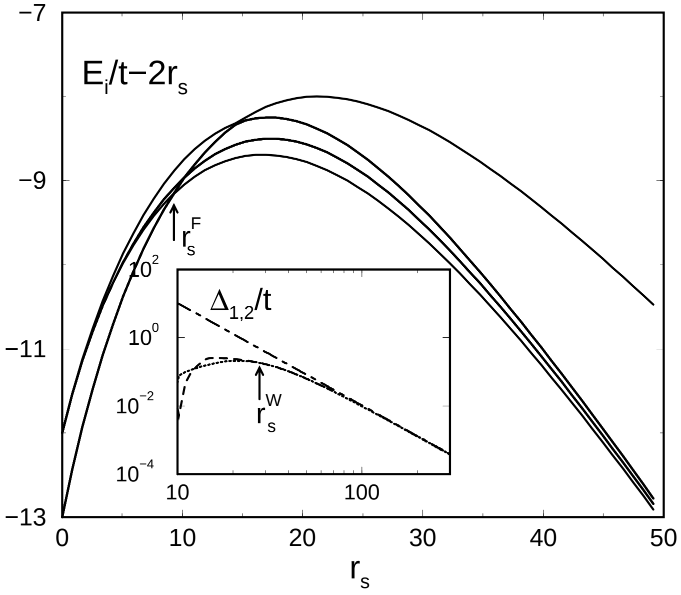

FIG. 1. As a function of r_s, low energy part of the spectrum exhibiting a level crossing at r_s^F. Inset: two first level spacings Δ_1/t (dashed) and Δ_2/t (dotted) and the perturbative result $3Dr_s^{-3}$ (dot-dashed).

The low energy part of the spectrum is shown in Fig. 1 as a function of r_s. If we follow the 4 GSs $E_0(r_s = 0)$ ($K_0 \neq 0$), one can see a first level crossing with a non degenerate state ($K_0 = 0$) which becomes the GS above r_s^F, followed by two other crossings with two other sets of 4 states with $K_I \neq 0$. When r_s is large, 9 states coming from $E_1(r_s = 0)$ have a smaller energy than the 4 states coming from $E_0(r_s = 0)$. The degeneracies ordered by increasing energy become $(1, 4, 4, 4)$ instead of $(4, 25, 64)$ for $r_s = 0$. Since the degeneracies are $(9, 36, 36)$ when $t = 0$, these 9 states give the 9 square molecules $|\Box_I>$ when $r_s \to \infty$. The centers of mass R_I of the $|\Box_I>$ are located on a periodic 3×3 square lattice. When r_s is large, one has a single massive molecule free to move on this restricted lattice, with a hopping term $T \propto tr_s^{-3}$ and quantized $K_l(I) = 2\pi p_l/3$ longitudinal and $K_t(I) = 2\pi p_t/3$ transverse momenta ($p_{l,t} = 1, 2, 3$). This gives 9 states of different kinetic energies given by $-2T(\cos K_l(I) + \cos K_t(I))$. The kinetic part of the low energy spectrum is then $-4T, -T, +2T$ with degeneracies $1, 4, 4$ respectively. This structure with two equal energy spacings Δ_1 and Δ_2 appears (inset of Fig. 1) when r_s is larger than the crystallization threshold r_s^W. Above r_s^W, to create a defect in the rigid molecule costs a high energy available in the 10^{th} excitation only.

To describe large r_s, one can use degenerate perturbation theory and study how the degeneracy of the 9 $|\Box_I>$ is removed by terms $\propto U/t \propto r_s^{-1}$. One obtains for the 9 low energy states:

$$\frac{E_I}{t} = E_D - 2\frac{T}{t}(\cos K_l(I) + \cos K_t(I)). \qquad (2)$$

$E_D = Ar_s + B/r_s + C/r_s^3$ and $T/t = D/r_s^3$ ($A \approx 2.13$, $B \approx -70.81$, $C \approx -18763.48$ and $D \approx 3463.97$). E_D comes from the small elastic vibrations of the rigid molecule while $8T$ is the band width of its zero point fluctuations.

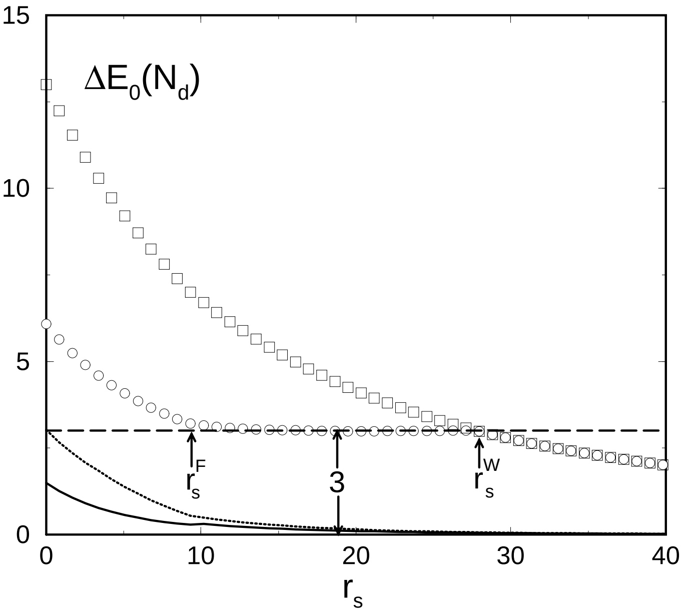

FIG. 2. Errors $\Delta E_0(N_d) = (E_0(N_d) - E_0)/t$ as a function of r_s: thick line ($d = 1$), dotted line ($d = \sqrt{2}$), circle ($d = 2$), square ($d = \sqrt{5}$).

The two thresholds r_s^F and r_s^W can be also detected if one calculates the GS energy $E_0(N_d)$ of the Hamiltonian truncated onto the N_d site SDs having a minimum inter-particle spacing $> d$. The difference $\Delta E_0(N_d) = (E_0(N_d) - E_0)/t$ between the GS of the truncated Hamiltonian and the exact GS is given in Fig. 2. $\Delta E_0(N_1)$ becomes negligible above r_s^F where the probability to have two nearest neighbor particles becomes weak. $\Delta E_0(N_{\sqrt{5}})$ coincides with $\Delta E_0(\square) = E_0(t = 0) - E_0$. The curve $\Delta E_0(N_2)$ is very remarkable. Above r_s^W, $\Delta E_0(N_2)$ is identical to $\Delta E_0(\square)$, while for $r_S^F < r_s < r_s^W$, $\Delta E_0(N_2) \approx 3$ independently of r_s. This suggests that the GS for intermediate r_s is composed of an elastic molecule, which can be projected onto the N_2 site SDs adapted to describe it, plus "excitations" having a nearly interaction independent kinetic energy $\approx -3t$, i.e. the energy of a particle at the Fermi surface of the non interacting system.

To understand further the nature of the intermediate GS, we have projected the GS wave functions $|\Psi_0(r_s)>$ over the two eigenbases valid for $U/t = 0$ (Fig. 3 upper left) and for $t/U = 0$ (Fig. 3 upper right) respectively. Below r_s^F, each of the 4 GSs $|\Psi_0^\alpha(r_s)>$ with $K_0 \neq 0$ has still a large projection

$$P_0(r_s) = \sum_{\beta=1}^{4} |<\Psi_0^\alpha(r_s)|K_0(\beta)>|^2 \qquad (3)$$

over the 4 non interacting GSs. There is no projection over the 25 first excitations and a small one $P_2(r_s)$ over the 64 second excitations of the non interacting system. Above r_s^F, the non degenerate GS with $K_0 = 0$ has a large projection

$$P_1(r_s) = \sum_{\beta=1}^{4} |<\Psi_0(r_s)|K_1(\beta)>|^2 \qquad (4)$$

which is equally distributed over the 4 excitations $|K_1(\beta)>$ of momentum $K_1 = 0$. Its projections onto the 4 $|K_0(\beta)>$, the 21 other first excitations and 64 second excitations of the non interacting system are zero. One concludes that a large part of the system remains an excited liquid above r_s^F, described by 4 equal projections onto the 4 $|K_1(\beta)>$. Those projections decrease as r_s increases.

The modulus $A(\square) = |<\square|\Psi_0(r_s)>|$ of the amplitude of the projection of the GS $|\Psi_0(r_s)>$ over a single square configuration $|\square>$ is given in Fig. 3 (upper right). $A(\square)$ does not depend on the chosen square and reaches 1/3 for large r_s, i.e. the value where the total projection over the 9 squares is equal to one. $A(\square)$ linearly increases when $r_s^F < r_s < r_s^W$ and gives $r_s \approx 37$ (the accepted value for $2d$ Wigner crystallization) by extrapolation. One concludes that a small but increasing part of the system begins to be a Wigner square molecule at r_s^F, described by 9 equal projections onto the $|\square_I>$. The site SDs and plane wave SDs are not orthonormal. After re-orthonormalization, the total projection p_t of $|\Psi_0(r_s)>$ over the subspace spanned by the 4 $|K_1(\beta)>$ and 9 $|\square_I>$ and P_t over the subspace spanned by the 4 $|K_1(\beta)>$ and 225 site SDs of lower electrostatic energies (9 squares, 36+36 parallelograms, 144 deformed squares) are given in an inset of Fig. 3 (upper right). One can see that $|\Psi_0(r_s)>$ mainly remains inside this small part of the large Hilbert space for intermediate r_s.

We consider now the GS response to small perturbations. The first one consists in piercing the $2d$ torus by an infinitesimal positive flux ϕ (periodic tranverse BCs, $t \rightarrow t\exp(i\phi/L)$ for longitudinal hopping only, $\phi = \pi$ corresponding to anti-periodic longitudinal BCs). The coefficients $a(r_s)$ and $b(r_s)$ (Kohn curvature) of the expansion $E_0(r_s, \phi) \approx E_0(r_s, 0) + a(r_s)\phi + b(r_s)\phi^2/2$ are given in Fig. 3 (lower right). When $r_s = 0$, ϕ removes the fourfold degeneracy of E_0, $a = -\sqrt{3}t/6$ and $b = 7t/36$. When r_s is large, the substitution $K_l(I) \rightarrow K_l(I) + 2\phi/3$ in Eq. 2 gives $a = 0$ and $b \approx 8Dtr_s^{-3}/9$. An infinitesimal positive flux ϕ gives rise to a persistent current

$I_l = -\partial E_0/\partial \phi = -a$ when $r_s < r_s^F$ while the GS curvature b exhibits a smooth crossover between two regimes around r_s^W (lower left inset of Fig. 3).

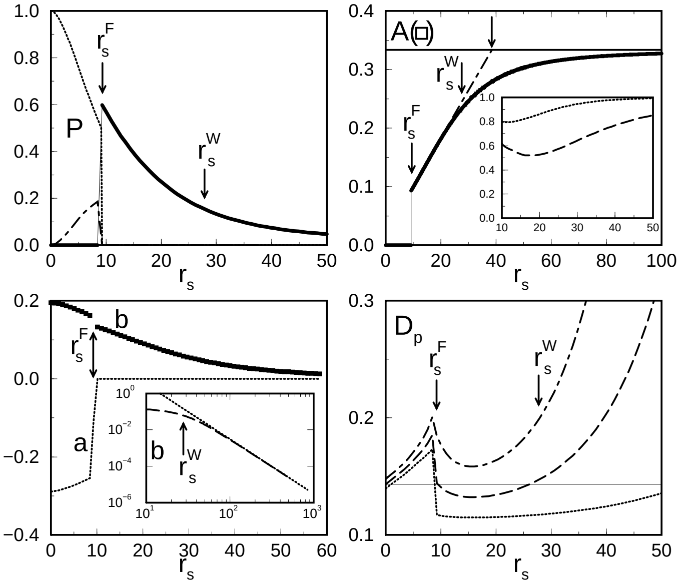

FIG. 3. As a function of r_s: Upper left: GS Projections P_O (dotted), P_1 (thick) and P_2 (dot-dashed) onto plane wave SDs; Upper right: GS Amplitude $A(\Box)$ (thick) over a single square site SD (the dot-dashed line reaches 1/3 at $r_s \approx 37$); Inset: GS Projection p_t (dashed) and P_T (dotted) over combined plane wave and site SD re-othonormalized bases; Lower left: $a(r_s)/t$ (dotted) and $b(r_s)/t$ (thick) characterizing the GS response to an infinitesimal flux; inset : $b(r_s)/t$ (dashed) and $8D/9r_s^{-3}$ (dotted); Lower right: GS density $D_p(r_s)$ at the pinning site with $V_p/t = -0.01$ (dotted), -0.05 (dashed) and -0.1 (dot-dashed).

The second perturbation consists in introducing a weak pinning well (negative potential V_p) at a single lattice site p. The GS density

$$D_p(r_s) =< \Psi_0(r_s)|c_p^\dagger c_p|\Psi_0(r_s) > \tag{5}$$

at the site p is shown in Fig. 3 (lower right). If $V_p = 0$, $D_p(r_s = 0) = 1/9$. A weak negative value of V_p yields a larger value for $D_p(r_s = 0)$. When one turns on the interaction, the effect is first enhanced and enhanced Friedel oscillations around p can be observed. At r_s^F, D_p drops and the interacting GS has a weaker response to a weak pinning well than the non interacting GS, as shown by the curves $D_p(r_s)$ and by the weaker Friedel oscillations observed around p. When r_s is large, D_p increases again and the Wigner molecule is pinned. This surprizingly weak response for intermediate r_s suggests that the system may very weakly respond to the presence of weak impurities.

From the study of the GS projections emerges the conclusion that a minimal description of the intermediate GS requires to combine the two limiting eigenbases. Instead of taking separately many low energy excitations of the $U/t = 0$ limit or of the $t/U = 0$ limit, one can use the subspace spanned by the 9 $|\Box_I >$ and the 4 $|K_1(0) >$ for having a large fraction of $|\Psi_0(r_s) >$ for intermediate r_s. In this sense, the GS is neither solid, nor liquid, but rather the quantum superposition of those two states of matter, as conjectured in Ref. [1]. This suggests possible improvements of the trial GS to use for intermediate r_s in variational quantum Monte Carlo approaches [6]. Instead of using Jastrow wave functions improving the plane wave SDs for the liquid or the site SDs for the solid, it will be interesting to study if a combination of the two describing a solid-liquid regime will not be better for intermediate r_s. This will confirm that an unnnoticed intermediate solid-liquid phase does exist in the thermodynamic limit for fermionic systems in two dimensions. This might help to explain the $2d$ metal observed in field effect devices. Eventually, our results for spinless fermions might also give a natural explanation for the competition between the Stoner ferromagnetism and the Wigner antiferromagnetism observed [12] for intermediate r_s when the spin degrees of freedom and the disorder are included.

We thank Boris Spivak for having drawn our attention on Ref. [1] and for discussions concerning Ref. [13]. This work is partially supported by a TMR network of the EU.

---

[1] A. F. Andreev and I. M. Lifshitz, Sov. Phys. JETP **29**, 1107 (1969).
[2] G. G. Batrouni and R. T. Scalettar, *Phys. Rev. Lett.* **84**, 1599 (2000).
[3] I. E. Dzyaloshinskii, P. S. Kondratenko and V. S. Levchenkov, Sov. Phys. JETP **35**, 823 (1972); ibid **35**, 1213 (1972).
[4] E. Abrahams, S. V. Kravchenko and M. P. Sarachik, cond-mat/0006055, to be published in Rev. Mod. Phys and refs therein.
[5] J. H. Schön, S. Berg, Ch. Kloc and B. Batlogg, Science **287**, 1022 (2000).
[6] B. Tanatar and D.M. Ceperley, *Phys. Rev.* B **39**, 5005 (1989).
[7] S.T. Chui and B. Tanatar, *Phys. Rev. Lett.* **74**, 458 (1995).
[8] G. Benenti, X. Waintal and J.-L. Pichard, *Phys. Rev. Lett.* **83**, 1826 (1999).
[9] G. Benenti, X. Waintal and J.-L. Pichard, *Europhys. lett.* **51**, 89 (2000).
[10] G. Benenti et al. in preparation.
[11] R. Berkovits and Y. Avishai, *Phys. Rev.* B **57**, R15076 (1998).
[12] F. Selva and J.-L. Pichard, cond-mat/0012015.
[13] B. Spivak, cond-mat/0005328.